Supplemental Information

MeCP2 Governs Maternal Hyperandrogenism-Induced Cortical Defects and Autism-like Behaviors via Noncanonical AR-Dependent Regulation of Mef2c

Yu-Meng Wang[1, 2, 7, *], Yanyan Jia[3, 7], Yu Wu[4, 5, 7], Qiaohang Zhao[5], Yu-Meng Guo[6], Li Zhang[1], Min Jin[5, *], Yu-Fang Zheng[2, 5, 8, *]

Correspondence: zhengyf@fudan.edu.cn (Y.-F. Z.), min_jin@zju.edu.cn (M. J.), yumeng1229@126.com (Y.-M. W)

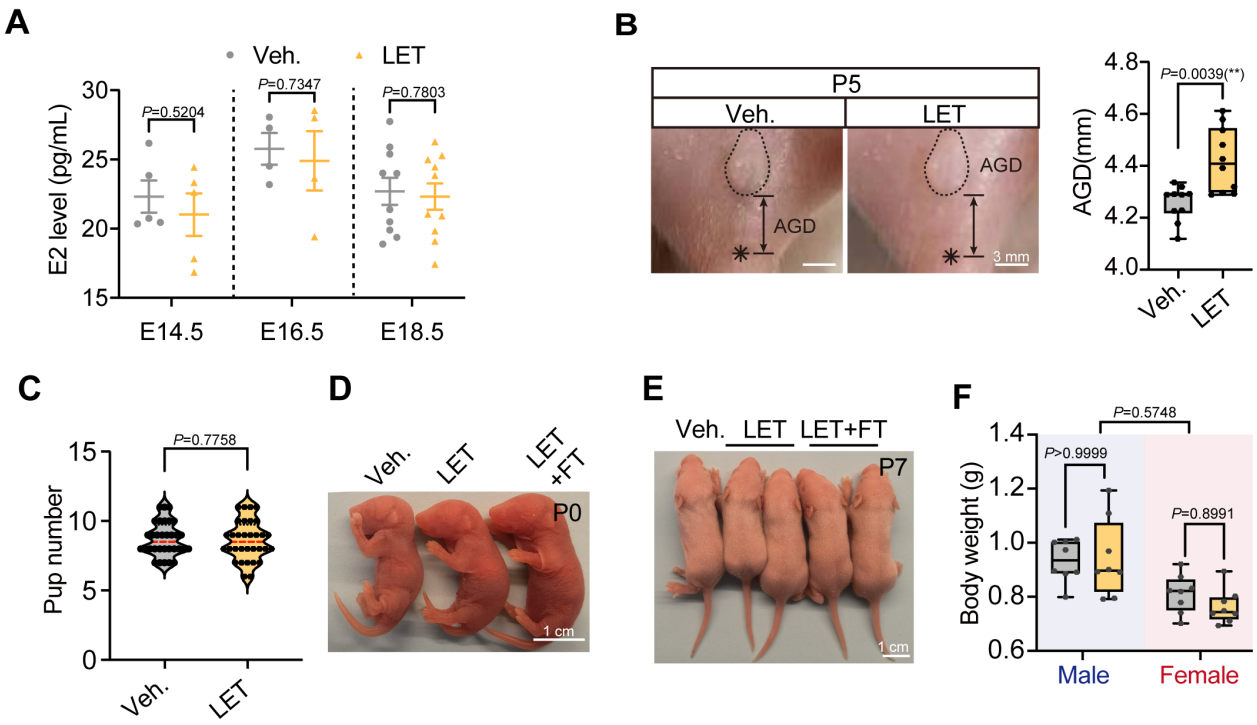

Figure S1

Figure S1. Prenatal hyperandrogen does not affect estradiol levels in pregnant mothers and has no effect on the overall growth and body weight of male offspring. (**A**) Quantification of the serum estradiol levels from the pregnant mice of the vehicle and letrozole-treated groups at different time points (N = 5 pregnant mice for E14.5, N = 4 pregnant mice for E16.5, and N = 10 pregnant mice for E18.5). (**B**) The effects of prenatal exposures on androgen activity in male offspring were determined by the anogenital distances (AGDs). The AGDs of the P5 male pups were longer in the letrozole-treated male offspring than those in the control group. N = 10 male offspring from 5 mothers for each group. (**C**) Quantification of the litter size of vehicle and letrozole-treated groups (N = 32 litters for each group). Appearance of male offsprings from vehicle, letrozole-treated, and letrozole plus flutamide-treated groups at P0 (**D**) and P7 (**E**). Scale bars, 1 cm. (**F**) Quantification of the body weight for male and female offspring at P7 in the vehicle and letrozole-treated groups (N = 8 males from 6 mothers for each group, N = 8 females from 6

mothers). Sex genotype interaction was not significant (ANOVA's interaction F = 0.3222). Veh.: vehicle; LET: letrozole; FT: flutamide. All data are expressed as the means ± SEM. Statistical analyses were performed with two-tailed unpaired Student's *t*-test (a-c) or two-way ANOVA test followed by Sidak *post-hoc* test. $^{**}P < 0.01$.

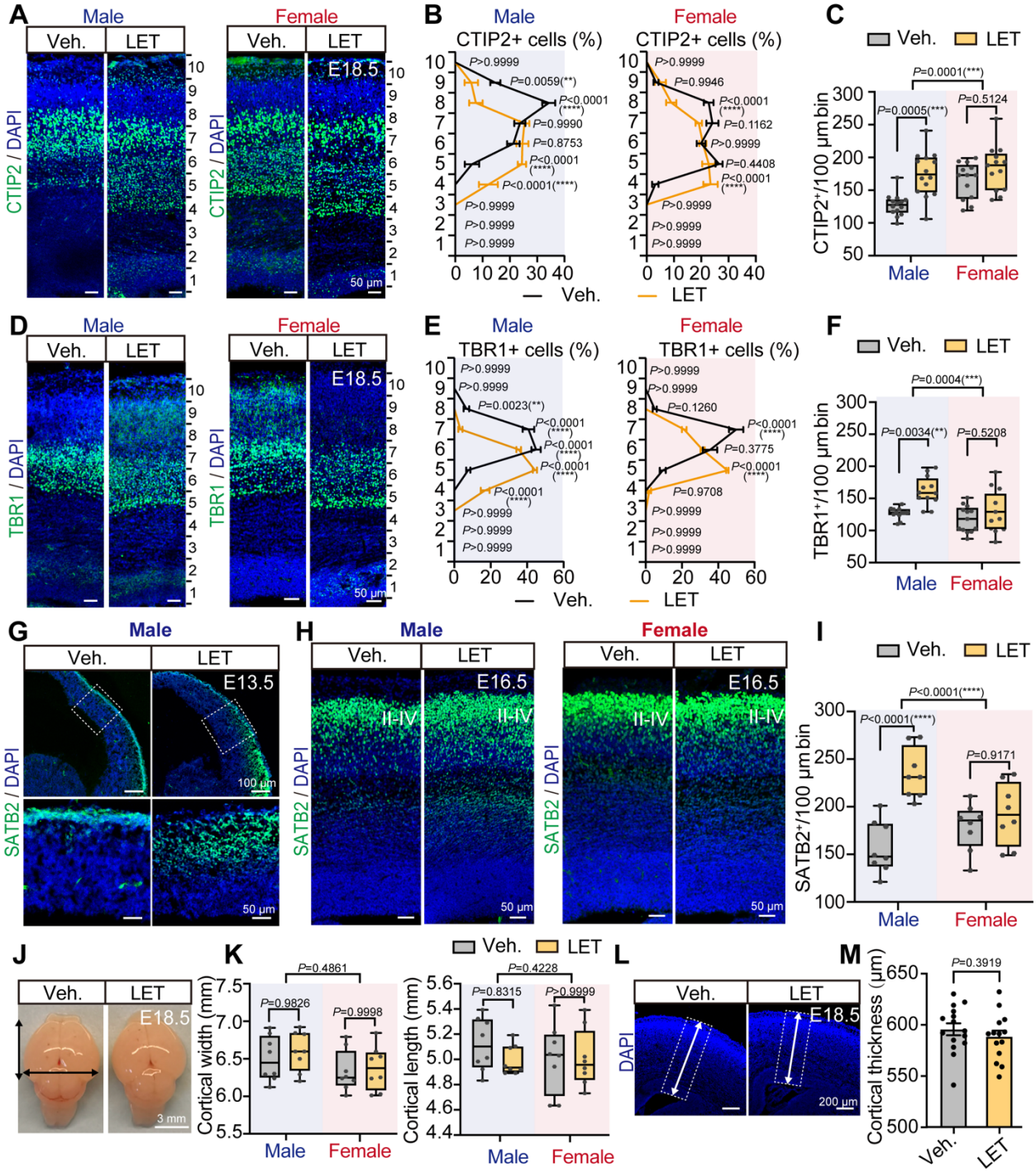

Figure S2

Figure S2. Maternal hyperandrogen exposure promotes cortical neurogenesis in offspring without affecting the overall size and weight of the brain. (**A-F**) Immunostaining of cortical

layer markers at E18.5. CTIP2 (layer V-VI) and TBR1 (layer VI) were labeled in green; nuclei were counterstained with DAPI (blue). The cortex was divided into 10 equal bins from the ventricular surface to the pial surface, and $CTIP2^+$ and $TBR1^+$ cells within 100 μm bins were quantified. Representative images (A, D) and bin-wise distribution of $CTIP2^+$ (E) and $TBR1^+$ (H) cells are shown (N = 6 per sex from 6 dams). Total $CTIP2^+$ (F; N = 14 males, 13 females from 6 dams) and $TBR1^+$ (I; N = 12 males, 13 females from 6 dams) cell counts showed significant sex × treatment interactions (ANOVA's interaction F = 17.27 and F = 14.33, respectively). (**G**) $SATB2^+$ cells were detected in cerebral cortices of male offspring at E13.5 from the vehicle and letrozole-treated groups. Scale bars: 100 μm. Regions in the white dotted boxes were displayed at a higher magnification (bottom panel). Scale bars: 50 μm. (**H-I**) $SATB2^+$ cells were detected in cerebral cortices of male (left) and female (right) offspring at E16.5 from the vehicle and letrozole-treated groups. Scale bars: 50 μm. N = 8 per sex from 6 dams per group. Significant sex × treatment interaction was observed (ANOVA's interaction F = 21). (**J-K**) Whole-brain images at E18.5 show gross cortical morphology; cortex length and width were quantified (K; N = 8 males from 6 dams per group). No significant sex × treatment interaction was detected for either measure (F = 0.4983 and F = 0.6619). Scale bar, 3 mm. (**L-M**) DAPI staining of coronal brain sections showing cortical thickness (L; black arrows). Quantification of thickness (M) was performed (N = 15 males from 10 dams). Scale bar, 200 μm. All data are expressed as the means ± SEM. Statistical analyses were performed with two-way ANOVA test followed by Sidak *post-hoc* test (C, E-F, H-I and K) or two-tailed unpaired Student's *t*-test (M). $^{**}P < 0.01$; $^{***}P < 0.001$; $^{****}P < 0.0001$.

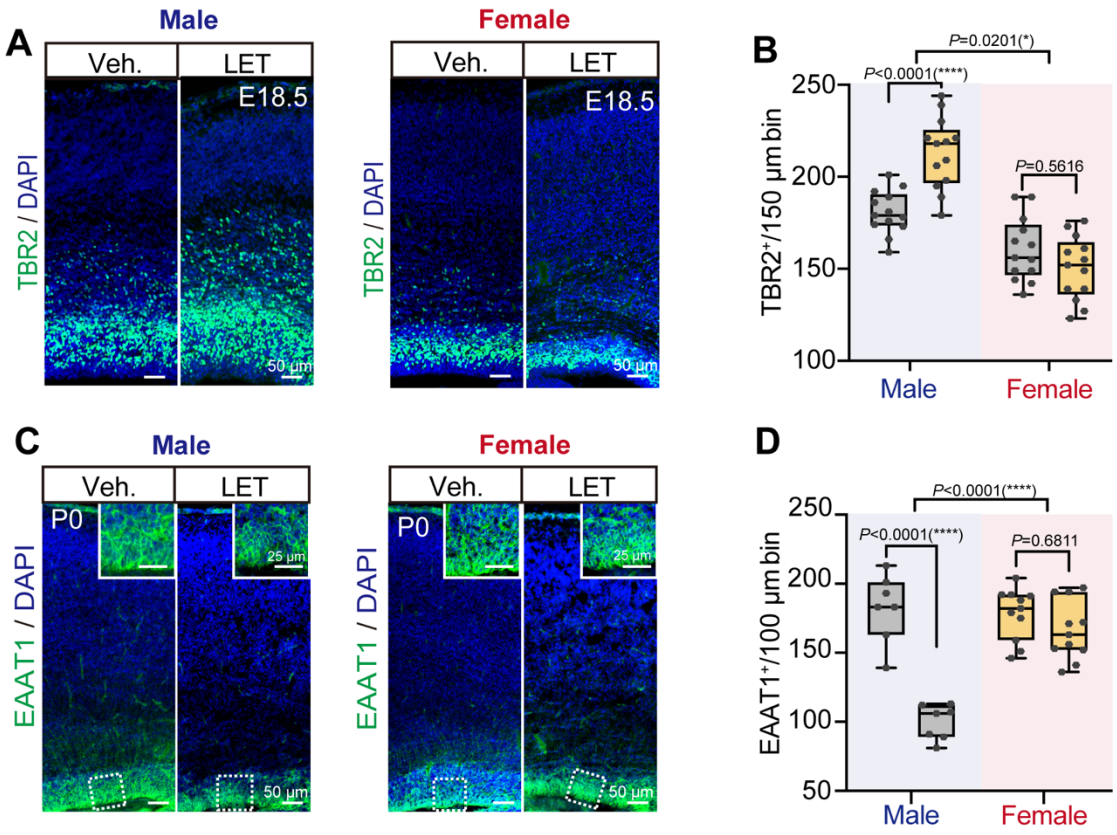

Figure S3

Figure S3. Maternal hyperandrogen exposure led to more intermediate progenitor cells and fewer astrocyte progenitor cells in male offspring. (**A-B**) TBR2$^+$ intermediate progenitor cells were detected in cortices at E18.5, and quantification of TBR2$^+$ cells per 150 μm bin was performed. Scale bars: 50 mm. N = 7 males from 5 mothers for vehicle-treated group, N = 6 males from 5 mothers for letrozole-treated group, N = 9 females from 5 mothers for each group. sex genotype interaction was significant (ANOVA's interaction F = 5.784). (**C-D**) Astrocyte progenitor cells were detected with EAAT1 staining in cerebral cortices at P0, and quantification of EAAT1$^+$ cells per 100 μm bin was performed. Scale bars: 50 μm. Regions in the white dotted boxes were displayed at a higher magnification on the top right corner. Scale bars: 25 μm. N = 7 male or female offspring from 5 mothers for each group. sex genotype interaction was significant

(ANOVA's interaction F = 47.80). All data are expressed as the means ± SEM. Statistical analyses were performed with two-way ANOVA test followed by Sidak *post-hoc* test. **P* < 0.05; *****P* < 0.0001.

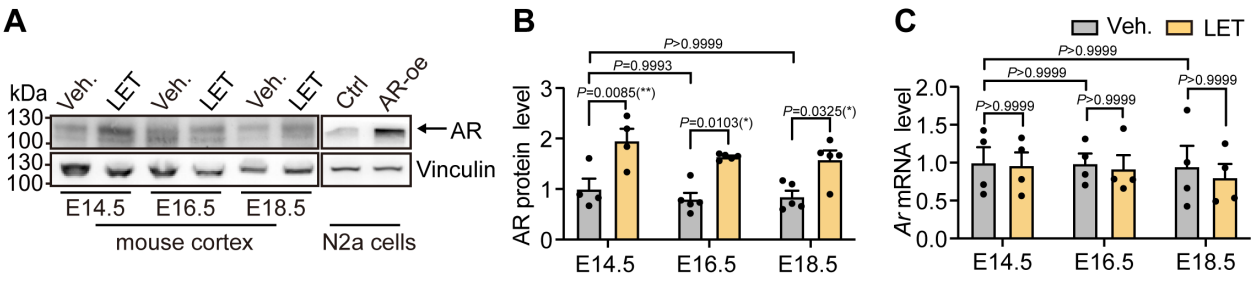

Figure S4

Figure S4. The expression of AR in the cerebral cortex of male offspring. (**A-B**) The protein levels of AR in male offspring. (A) Cerebral cortices were collected from male offspring of the vehicle (Veh.) and letrozole (LET) treated groups at E14.5 (N = 4 male offspring from 4 mothers), E16.5 (N = 5 male offspring from 4 mothers), and E18.5 (N = 5 male offspring from 4 mothers). AR protein levels were evaluated by western blot, with Vinculin used as the loading control. AR overexpression in N2a cells were used as positive control. Quantification of AR in cortices was shown in (B). Data were normalized to the averaged levels of vehicle-treated samples. (**C**) The mRNA levels of AR in cerebral cortices. N = 4 male offspring from 4 mothers for each group. All data are expressed as the means ± SEM. Two-way ANOVA followed by Sidak *post-hoc* test was performed for B-C. **P* < 0.05, ***P* < 0.01.

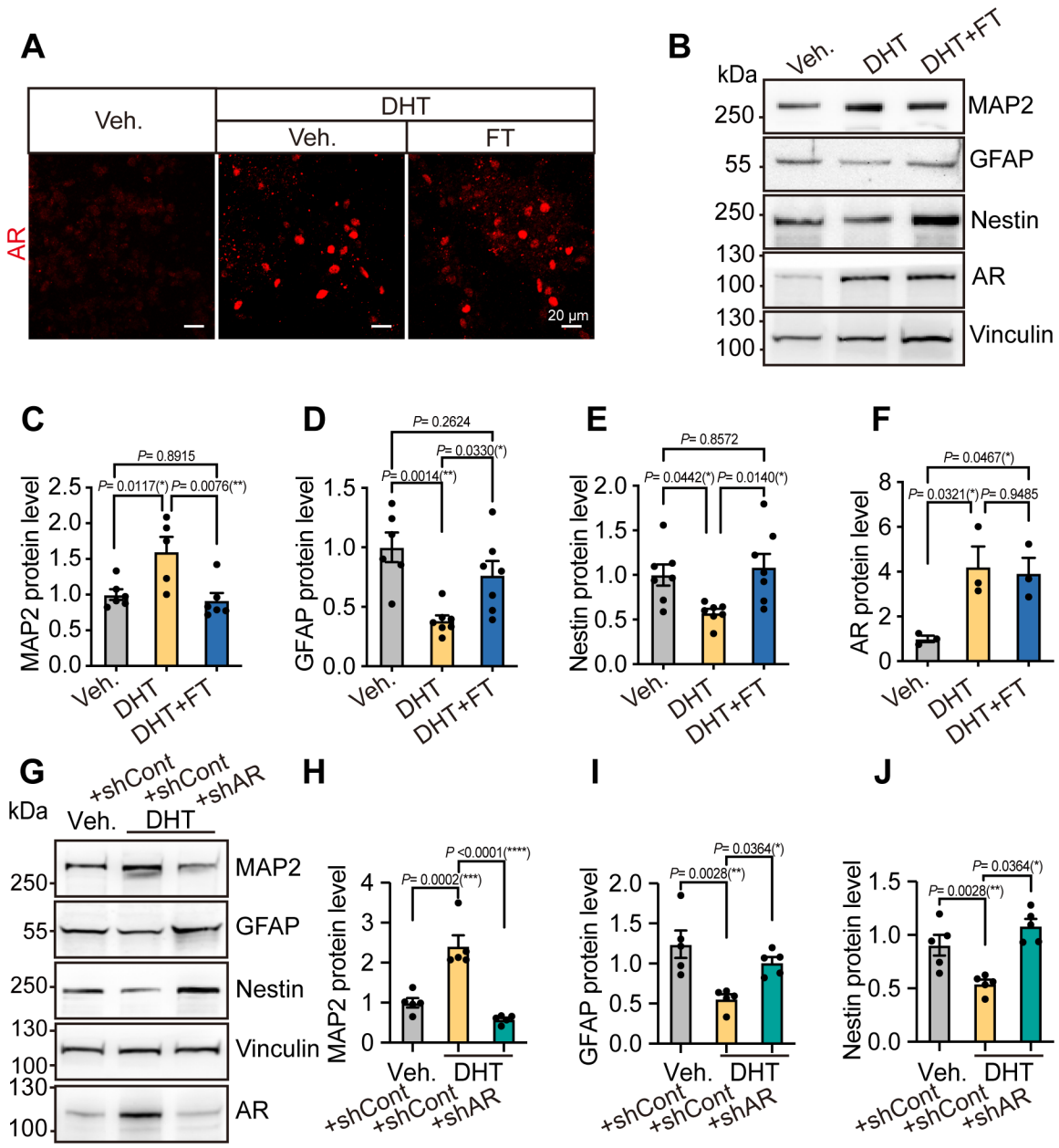

Figure S5

Figure S5. Hyperandrogen promotes cortical neurogenesis and inhibits gliogenesis in cultured mouse primary NPCs. (**A-F**) Cultured mouse primary NPCs were treated with vehicle (Veh.), DHT (10 nM), or DHT plus flutamide (FT). Representative images of immunofluorescent staining (A), western blot (B), and quantifications (C-F) for MAP2 (N = 6 for veh. group and DHT

+ FT group; N = 5 for DHT group), GFAP (N = 6 for veh. group; N = 7 for DHT group and DHT + FT group), Nestin (N = 7 for each group), and AR (N = 3 for each group) are shown, respectively. Scale bars: 20 μm. Mouse Vinculin was used as the loading control. Data were normalized to the averaged levels of vehicle-treated samples. (**G-J**) Cultured mouse primary NPCs were treated with vehicle (Veh.), or DHT (10 nM) and then infected with lentivirus (shCont or sh- Ar). Western blot analysis was performed for GFAP, MAP2, Nestin and AR (N = 5 independent experiments). Vinculin was used as loading control. All data are expressed as the means ± SEM. Statistical analyses were performed with one-way ANOVA test followed by Tukey *post-hoc* test. **P* < 0.05; ***P* < 0.01; ****P* < 0.001; *****P* < 0.0001.

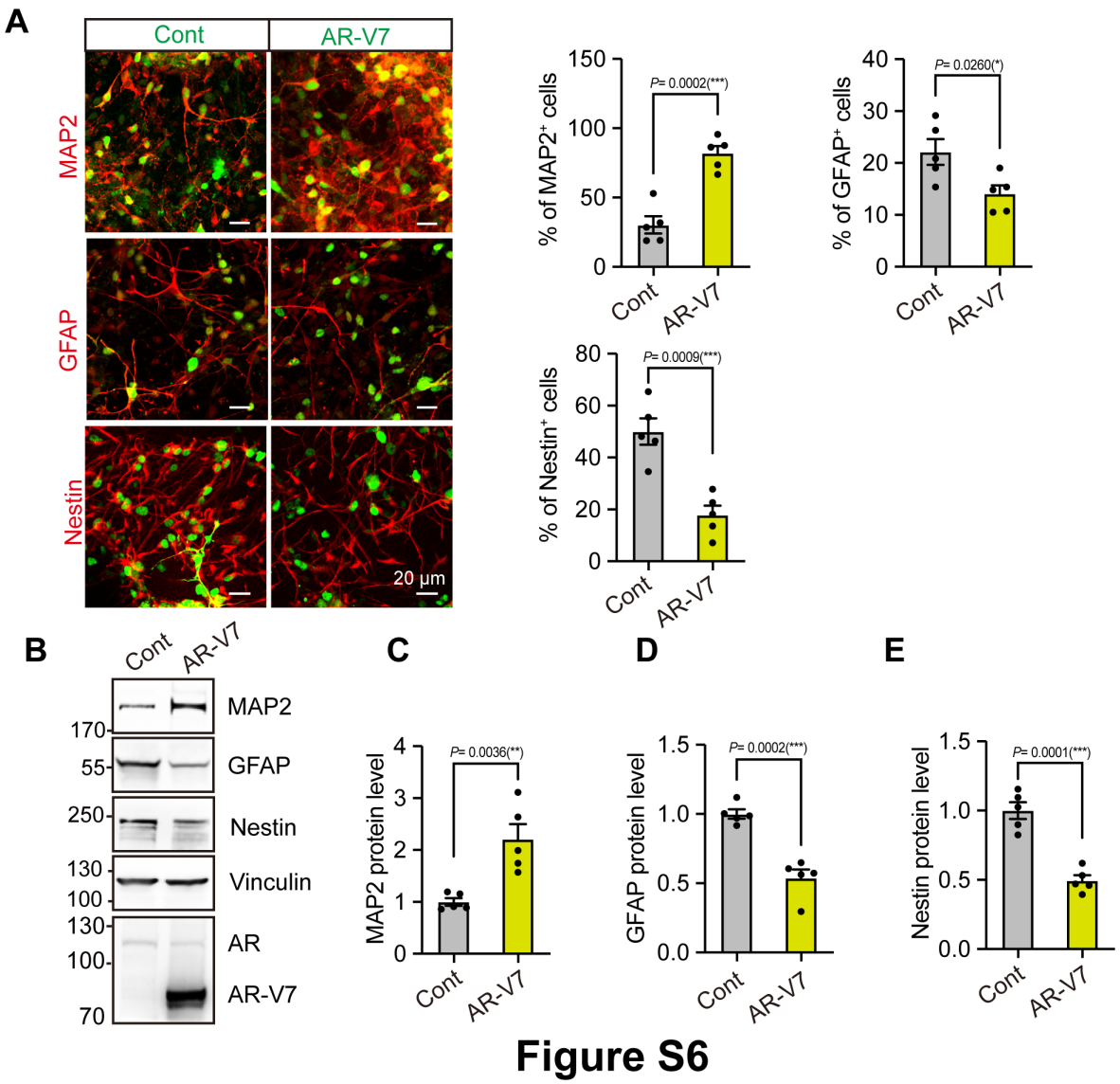

Figure S6

Figure S6. Overexpression the constitutively active form of AR (AR-V7) promotes cortical neurogenesis and inhibits gliogenesis in cultured mouse primary NPCs. (**A-E**) Cultured mouse primary NPCs were infected with lentivirus (Cont or AR-V7). Representative images of immunofluorescent staining (A) and western blot (B) and quantifications (C-E) for MAP2, GFAP and Nestin are shown, respectively. Scale bars: 20 μm. Mouse Vinculin was used as the loading control. Data were normalized to the averaged levels of cont- virus infected samples. N = 5 independent experiments. All data are expressed as the means ± SEM. Statistical analyses were performed with two-tailed unpaired Student's *t*-test. **P* < 0.05; ***P* < 0.01; ****P* < 0.001.

Overlapped genes assosiatied with ASD (regulated genes, |log(FC)|>0.3)

Gene Name	Related diseases (MalaCards)	Genes involved in ASD		AR-bound genes
		SFARI	ASD-DEG	
MEF2C	Neurodevelopmental disorder ; autism spectrum disorder	Yes	Yes	Yes
NR3C2	Pseudohypoaldosteronism	No	Yes	No
CAV2	Lung pleomorphic carcinoma; Brill-Zinsser disease	No	No	
NT5E	Calcification of joints and Arteries; Periarthritis	No	No	Yes
MLIP	Myopathy with myalgia; Ocular hypertension	No	No	No
SLC35F4	Spinocerebellar ataxia; Adult-onset severe asthma	No	No	No
BHLHE22	Hermansky-Pudlak Syndrome	No	Yes	No
CCPG1	Encephalopathy; hereditary sensory; autonomic neuropathy	No	No	No
OTOGL	Deafness	No	No	No
OSMR	Amyloidosis; Primary cutaneous amyloidosis	No	No	Yes
CREBL2	Temtamy syndrome; Cantu syndrome	No	No	No
COL1A1	Caffey disease; Osteogenesis imperfecta	No	Yes	No
CASP1	Cowpox; Shigellosis	No	Yes	Yes
CYTH4	/	No	Yes	No
TULP2	Retinitis pigmentosa; Retinal degeneration	No	No	Yes
NR5A1	46,Xx sex reversal; Premature ovarian failure	No	Yes	Yes
PRDM13	Cerebellar dysfunction; Hypogonadotropic hypogonadism	No	No	No
FOXB1	Wernicke-Korsakoff syndrome; Thiamine deficiency disease	No	No	No
GPR179	Night Blindness	No	No	Yes
OTP	Pulmonary neuroendocrine tumor	No	No	No
FAM181B	Nephronophthisis	No	No	Yes
ECEL1	Arthrogryposis; Primary optic atrophy	No	No	No
H1F0	Hyperoxaluria	No	No	No
NDUFAF8	Mitochondrial Disease	No	No	No
SOX3	Intellectual developmental disorder; Panhypopituitarism	No	No	Yes
CHRAC1	Autosomal recessive intellectual developmental disorder	No	No	No

Figure S7

Figure S7. Screening the targets of AR during cortex development. The gene listed here are those shared DEGs identified in two datasets: our RNA-seq data and a published RNA-seq data

using human neural stem cells (hNSCs) treated with DHT (19). AR bound genes are based on recently published ChIP-seq datasets (19, 38). Related diseases information is from MalaCards-human disease database (55). SFARI refers to the Simons Foundation Autism Research Initiative Gene database. ASD-DEGs refers to genes differentially expressed between individuals with autism spectrum disorders (ASD) and controls.

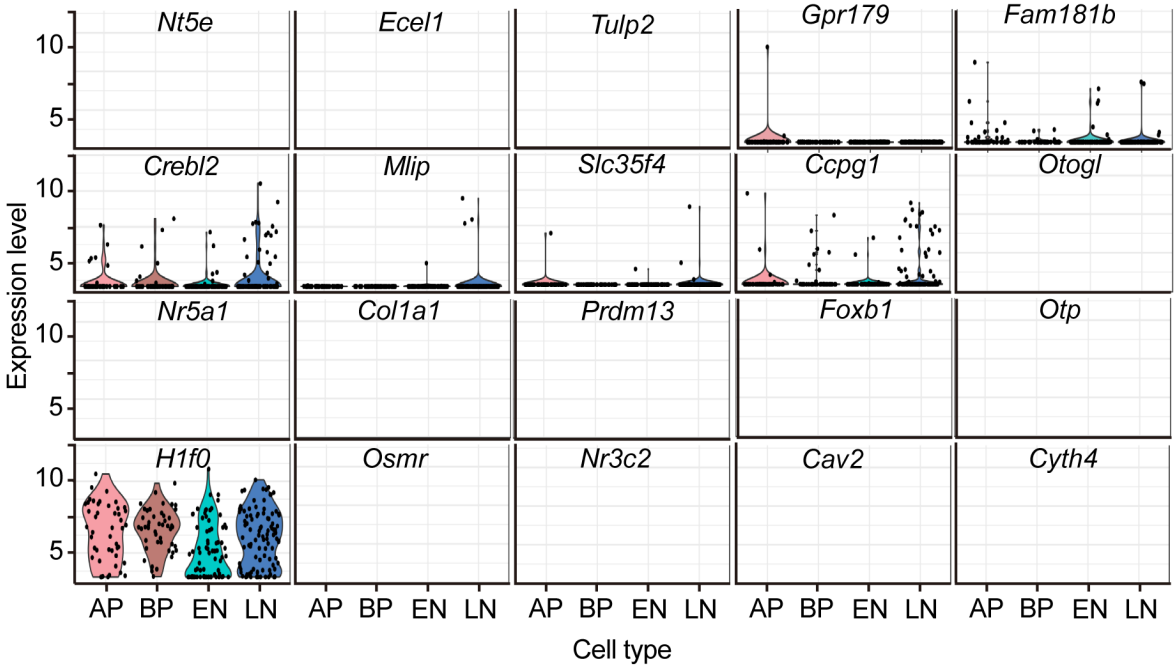

Figure S8

Figure S8. The expression patterns of 20 selected AR-targeted genes during cortical development. Data were extracted from a published single-cell RNA-sequencing dataset of radial glial cells (RGCs) and their progeny (54).

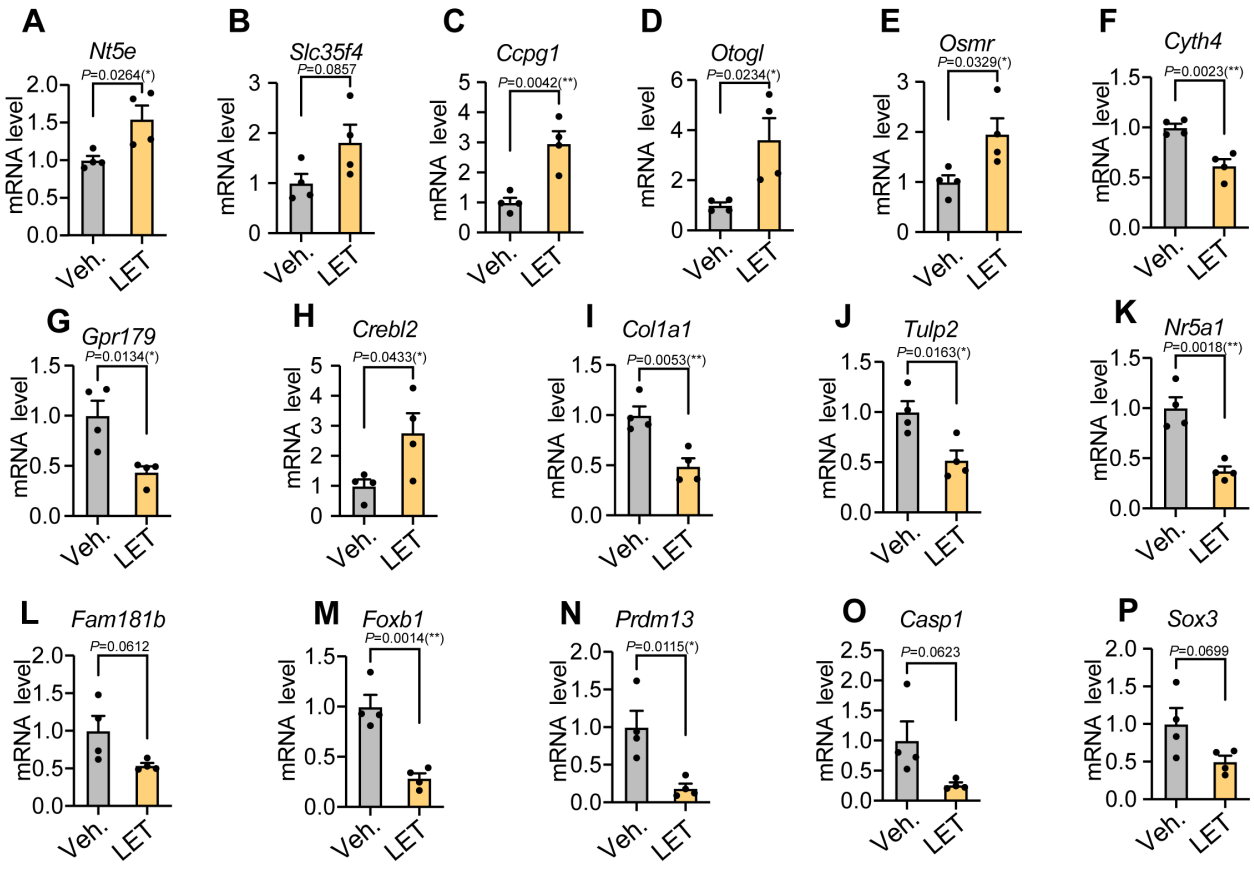

Figure S9

Figure S9. RT-PCR validation of DE genes from RNA-seq. (**A-P**) The mRNA level of 18 DE genes in vehicle (Veh.) vs letrozole (LET) treated embryonic cerebral cortex at E17.5 (N = 4 male offspring from 4 mothers in each group) were confirmed by qRT-PCR. All *Ct* values were first normalized to *Gapdh* control. The ratio (letrozole over vehicle) was calculated for each experiment and data are expressed as the means ± SEM. **P* < 0.05; ***P* < 0.01. Unpaired Student's *t* test was performed.

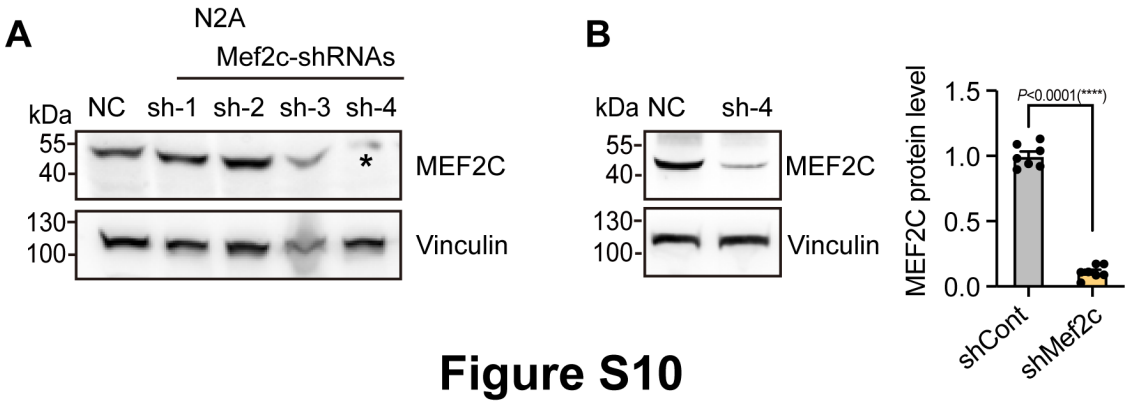

Figure S10

Figure S10. *Mef2c* shRNAs knockdown efficiencies were assessed by western blot. (**A**)The protein level of MEF2C was detected in N2a cells transfected with control or different *Mef2c* shRNAs. Mouse Vinculin was used as the loading control. * Mef2c-shRNA4 was the most efficient shRNA. (**B**) The protein level of MEF2C was detected in mouse primary NPCs infected with lentivirus (control or *Mef2c* shRNA4). Mouse Vinculin was used as the loading control. N = 7. Data are expressed as the means ± SEM. Statistical analyses were performed with two-tailed unpaired Student's *t*-test. ****$P < 0.0001$.

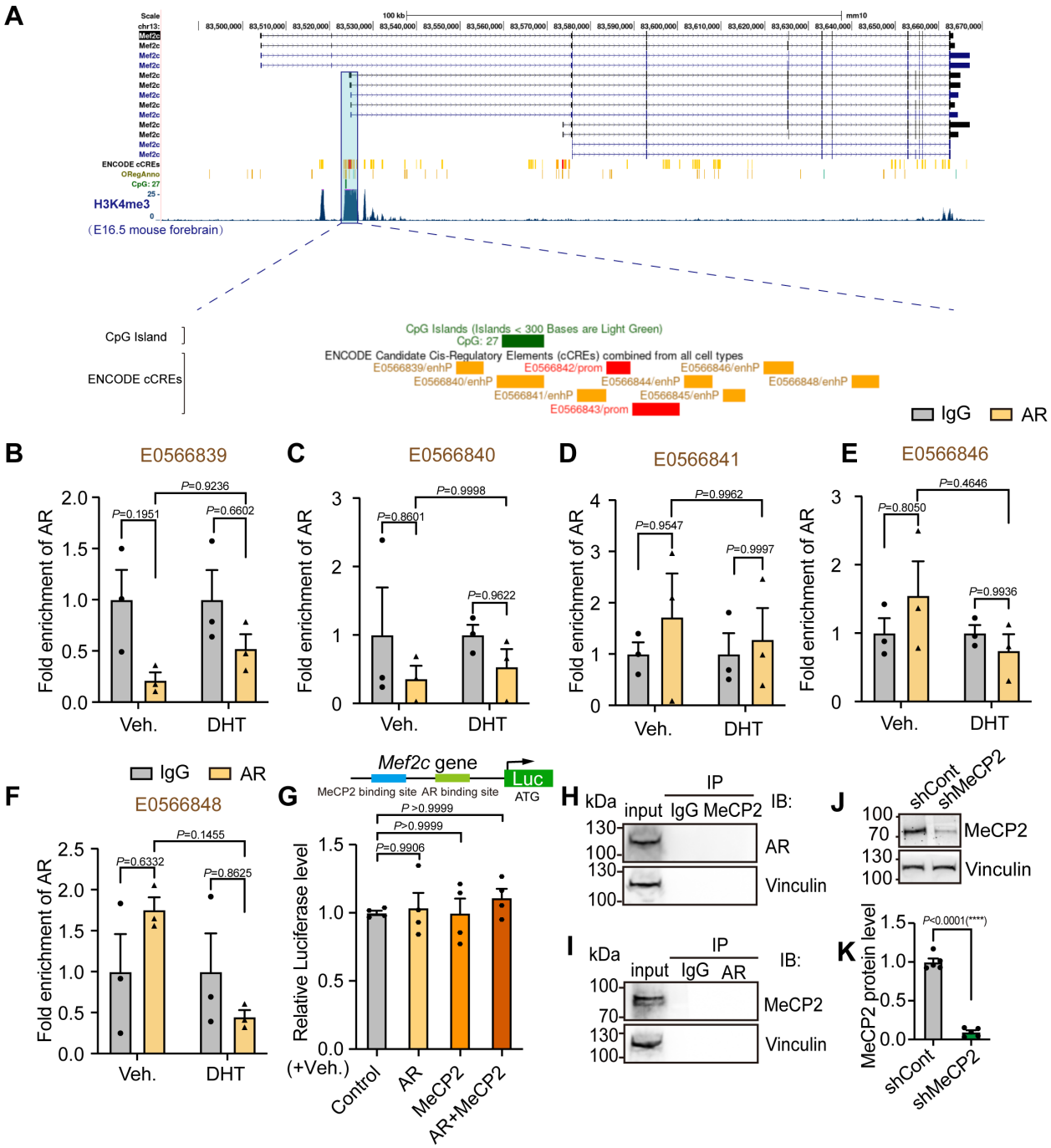

Figure S11

Figure S11. Identification of AR binding sites on mouse *Mef2c* gene by sequence analysis and ChIP-qPCR. (**A**) Schematic illustration of the position of CpG island (green), promoters (red) and proximal enhancer (orange) of *Mef2c* gene. Adapted from UCSC Genome Browser. (**B-F**) N2a

cells were treated with vehicle or DHT. ChIP-qPCR was performed to analyze the relative enrichment of AR in *Mef2c* promoters (E0566839 (B), E0566840 (C), E0566841 (D), E0566846 (E), and E0566848 (F)) in chromatin by using the AR antibodies or control IgG. N = 3 independent experiments. (**G**) Luciferase activities of the empty vector- (CONT), MeCP2-, AR- or MeCP2 plus AR- transfected N2a cells co-expressing the pGL3-*Mef2c*-WT luciferase reporter. The pGL3-*Mef2c*-WT luciferase reporter encompasses predicted AR binding site and MeCP2 binding site of the *Mef2c* gene. Diagram of the luciferase reporter is indicated in the upper panel. N = 4 independent experiments. (**H-I**) Co-immunoprecipitation assay between MeCP2 and AR. N2a cells were transfected with MeCP2 and AR, and whole cell lysates were immunoprecipitated with anti-MeCP2 (K) or anti-AR (I), then subjected to immunoblot analysis with anti-AR, anti-MeCP2 or anti-Vinculin. Vinculin, negative control. (**J-K**) MeCP2 shRNAs knockdown efficiencies were assessed by western blot. The protein level of MeCP2 was detected in mouse primary NPCs infected with lentivirus (control or *Mecp2* shRNA). Mouse Vinculin was used as the loading control. N = 5. All data are expressed as the means ± SEM. Two-way ANOVA followed by Sidak *post-hoc* test was performed for B-F. One-way ANOVA followed by Tukey *post-hoc* test was performed for G. Two-tailed unpaired Student's *t* test was performed for K.

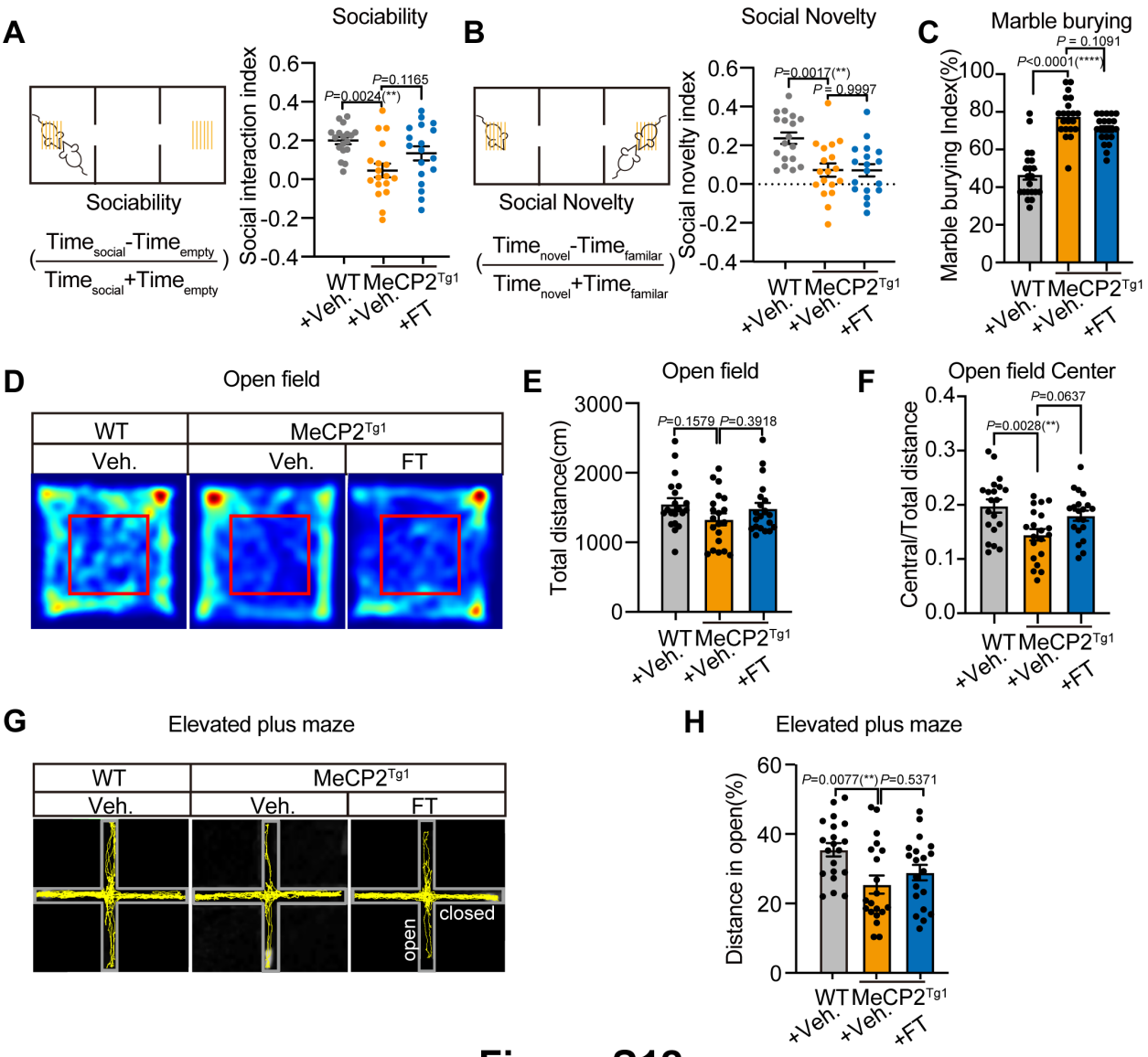

Figure S12

Figure S12. Flutamide fails to rescue autism-like behaviors in female MeCP2^{Tg1} mice. (**A-B**) Three-chamber social interaction (A) and social novelty (B) tests. Diagrams (left) and quantification (right) are shown. Control group: 18 female offspring from 10 dams; letrozole group: 18 females from 10 dams. (**C**) Marble burying index, calculated as the proportion of buried marbles (N = 21 females from 10 dams per group). (**D-F**) Open field test: representative locomotor heatmaps (D), total distance traveled (E), and center/total distance ratio (F), N = 20 females from

10 dams per group. (**G-H**) Elevated plus maze test: representative locomotion tracks (G) and quantification of open arm distance (H) (N = 20 females from 10 dams per group). Data are presented as mean ± SEM. Statistical analyses were performed with two-way ANOVA test followed by Sidak *post-hoc* test for (B) . One-way ANOVA followed by Tukey *post-hoc* test was performed for (A-C), (E-F) and (H). **P* < 0.05; ***P* < 0.01; ****P* < 0.001; *****P* < 0.0001.

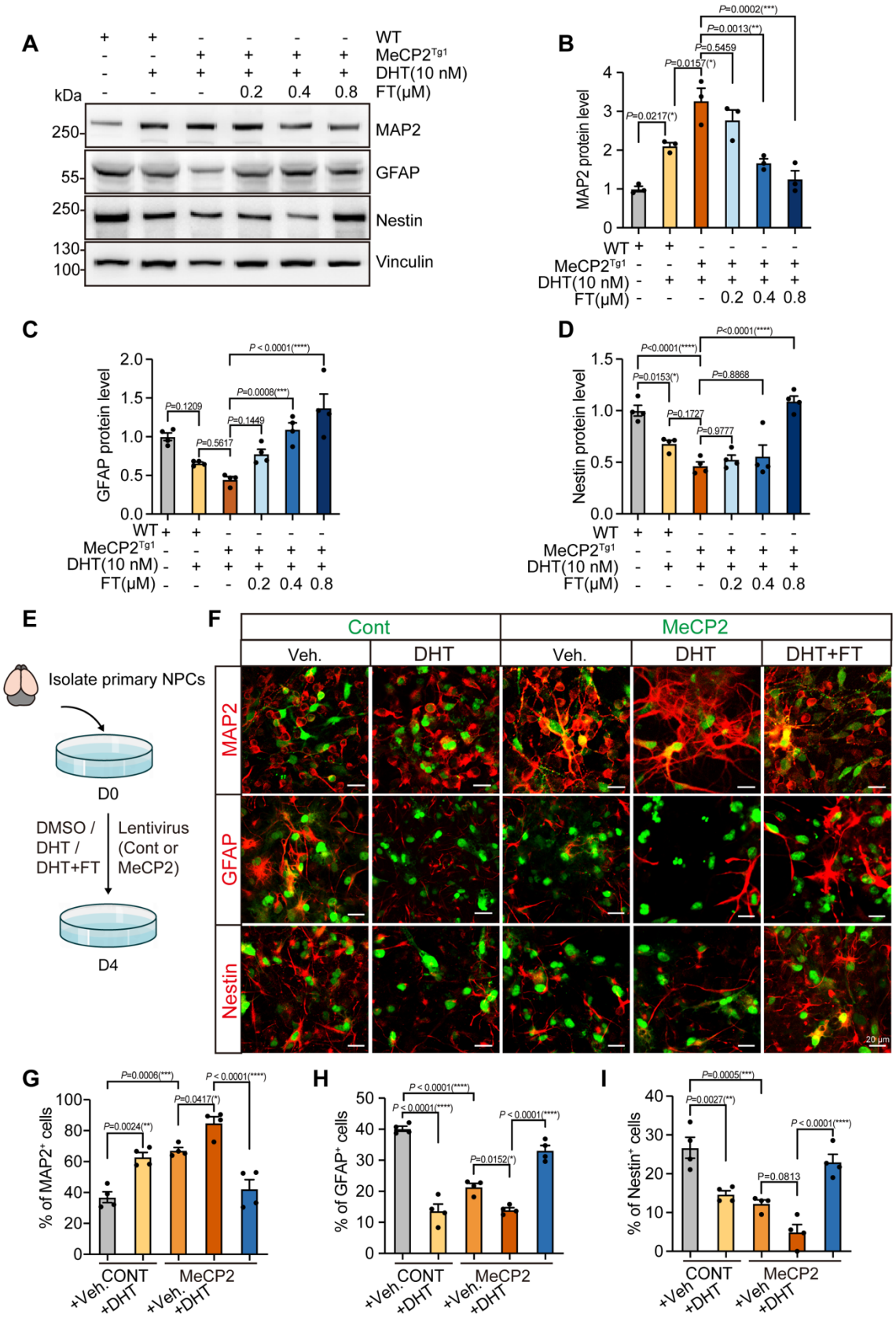
A
WT
MeCP2Tg1
DHT(10 nM)
FT(μM)
kDa
250
MAP2
55
GFAP
250
Nestin
130
100
Vinculin
B
MAP2 protein level
P=0.0217(*)
P=0.0157(*)
P=0.5459
P=0.0013(**)
P=0.0002(***)
C
GFAP protein level
P=0.1209
P=0.5617
P=0.1449
P=0.0008(***)
P < 0.0001(****)
D
Nestin protein level
P=0.0153(*)
P<0.0001(****)
P=0.1727
P=0.9777
P=0.8868
P<0.0001(****)
E
Isolate primary NPCs
D0
DMSO / DHT / DHT+FT
Lentivirus (Cont or MeCP2)
D4
F
Cont
MeCP2
Veh.
DHT
Veh.
DHT
DHT+FT
MAP2
GFAP
Nestin
20 μm
G
% of MAP2+ cells
P=0.0024(**)
P=0.0006(***)
P=0.0417(*)
P < 0.0001(****)
CONT
MeCP2
+Veh.
+DHT
H
% of GFAP+ cells
P < 0.0001(****)
P < 0.0001(****)
P=0.0152(*)
P < 0.0001(****)
I
% of Nestin+ cells
P=0.0027(**)
P=0.0005(***)
P=0.0813
P < 0.0001(****)

Figure S13

Figure S13. Blocking AR rescues the enhanced cortical neurogenesis caused by MeCP2 overexpression. (**A-D**) Primary NPCs were isolated from WT or MeCP2^{Tg1} male mouse at E14.5 and then treated with DMSO (Veh.), DHT (10 nM), or DHT plus different concentrations of flutamide (FT) (0.2, 0.4 or 0.6 μM). Western blot for MAP2, GFAP, and Nestin was performed. Representative pictures were displayed in (A) and quantification for each marker were shown in (b-d), respectively (N = 3 for B, N = 4 for C and D). Data were normalized to the averaged levels of vehicle-treated samples from WT mouse primary NPCs. Mouse Vinculin was used as the loading control. (**E**) Schematic of the experiment workflow in primary NPCs with DHT treatment. (**F-J**) Immunofluorescent staining for MAP2, GFAP, and Nestin were performed on NPCs. Representative images are shown in (F, scale bars: 20 μm), and quantifications for each marker are shown in (G-J), respectively (N = 4 independent experiments). Data were normalized to the averaged levels of vehicle-treated samples. All data are expressed as the means ± SEM. Statistical analyses were performed with one-way ANOVA test followed by Turkey *post-hoc* test. **P* < 0.05; ***P* < 0.01; ****P* < 0.001; *****P* < 0.0001.

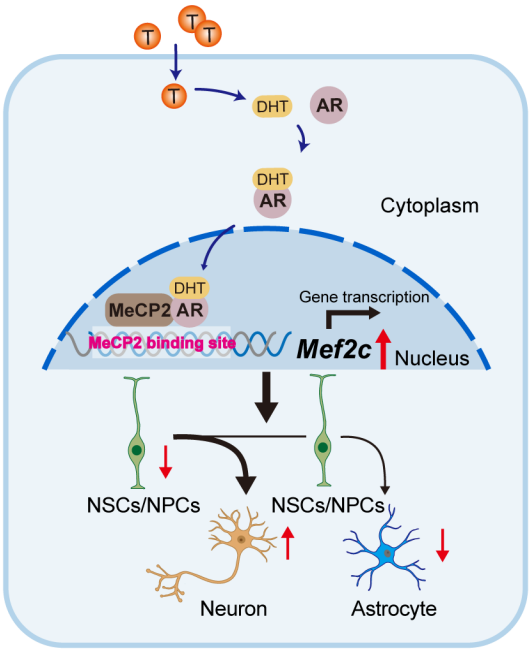

Figure S14

Figure S14. Schematic illustration of the regulation of Mef2c by AR in a MeCP2-dependent manner during cortical neurogenesis.

Table S1 The primers used for qRT-PCR and sex identification.

Gene name	Primer
Mouse *Gapdh*	F: 5'- ACAGCAACTCCCACTCTTCCACCT -3'
	R: 5'- TTGCTCAGTGTCCTTGCTGGGG -3'
Mouse *Mef2c*	F: 5'- ATCCCGATGCAGACGATTCAG -3'
	R: 5'- GGTTGAGGTAGGCGACTAAGC -3'
Mouse *Bhlhe22*	F: 5'- TCTGTGAACGGAGCGGTG -3'
	R: 5'- CTTACTCAGGCGGCCTCC -3'
Mouse *Ndufaf8*	F: 5'- CTGTAACATGGAAACTGGGGAAA -3'
	R: 5'- CCATAGCTGAACTGAAAACCACC -3'
Mouse *Chrac1*	F: 5'- GCCGTGGGGAAGGAAAAGT -3'
	R: 5'- CTCCTGGTTGATGCTCGACA -3'
Mouse Sry	F: 5'- TTTTACAGCCTGCAGTTGCC -3'
	R: 5'- ATGTGATGGCATGTGGGTTC -3'
Mouse *Nr3c2*	F: 5'- GAAAGGCGCTGGAGTCAAGT -3'
	R: 5'- TGTTCGGAGTAGCACCGGAA -3'
Mouse *Cav2*	F: 5'- TCACCAGCTCAACTCTCATCT -3'
	R: 5'- GCCAGAAATACGGTCAGGAACT -3'
Mouse *Nt5e*	F: 5'- GGACATTTGACCTCGTCCAAT -3'
	R: 5'- GGGCACTCGACACTTGGTG -3'
Mouse *Slc35f4*	F: 5'- GGCAGAAGTAATAATGGCCGAT -3'
	R: 5'- CCGAGCCCTCTCAATGTGG -3'
Mouse *Ccpg1*	F: 5'- AGGAATCCAGTAGCGATGACA -3'
	R: 5'- CTAAAGTGGCGTTTACTTGGCT -3'
Mouse *Otogl*	F: 5'- AGTTTGAAGCAACCTCTCCGA -3'
	R: 5'- AACAGAAAGCCCCGTTAAGGC -3'
Mouse *Osmr*	F: 5'- CATCCCGAAGCGAAGTCTTGG -3'
	R: 5'- GGCTGGGACAGTCCATTCTAAA-3'
Mouse *Crebl2*	F: 5'- CGGAAGCCAGCCAAAATCG -3'
	R: 5'- CGACTGGATACCAACTCCTCC -3'
Mouse *Col1a1*	F: 5'- GCTCCTCTTAGGGGCCACT -3'
	R: 5'- CCACGTCTCACCATTGGGG -3'
Mouse *Casp1*	F: 5'- ACAAGGCACGGGACCTATG -3'
	R: 5'- TCCCAGTCAGTCCTGGAAATG -3'
Mouse *Cyth4*	F: 5'- TACAGCAGATCAAATGGCACAG -3'
	R: 5'- GCCCTTATTAGGGTCCATGTTG -3'
Mouse *Tulp2*	F: 5'- AAGTGGAGCGTCTCAGGAGAA -3'
	R: 5'- CAAATAGCTGTCGCTGTTGTTC -3'

Mouse *Nr5a1*	F: 5'- CCCAAGAGTTAGTGCTCCAGT -3'
	R: 5'- CTGGGCGTCCTTTACGAGG -3'
Mouse *Prdm13*	F: 5'- ACTCTGGAAGCTATTGCAGACT -3'
	R: 5'- GTTGTAGGGATGTCAAACCACTG -3'
Mouse *Foxb1*	F: 5'- CTTCAAGGTGCTCAAGTCAGAC -3'
	R: 5'- GTTCTCGATAGCAAAGGGATGC -3'
Mouse *Gpr179*	F: 5'- CACTACCGTCCCAAGCCAAG -3'
	R: 5'- TGACAGCCGTTGAACATCTCC -3'
Mouse *Fam181b*	F: 5'- CAGTGGCAACGATTCGGGT -3'
	R: 5'- GGCTCGGGGTATAGTAGGTTC -3'
Mouse *Sox3*	F: 5'- GCCGACTGGAAACTGCTGA -3'
	R: 5'- CGTAGCGGTGCATCTGAGG -3'

Table S2 The primers used for ChIP-qPCR.

Positions in *Mef2c* promoter	**Primer**
Mouse *Mef2c*-MeCP2 binding site	F: 5'- CACTTGAGCACACGCGTACA -3'
	R: 5'- ACCCACACAGAACCTTCAAAGTC -3'
Mouse *Mef2c*-AR binding site	F: 5'- AATTCACATCTGACTCTTCCTGT -3'
	R: 5'- AAGACAGCGACTTCAAGGTC -3'

Table S3 The sequences of different regions of mouse *Mef2c*-promoter.

***Mef2c* promoter truncations**	**Sequence**
Mef2c-WT	ACACTTCGTCTCCAGCTCTCTGCTCGCTCGCCTCGCAGTCACAGACACT TGAGCACACGCGTACACCCAGACATCTTCGGGCTGCTATTGGATTGACT TTGAAGGTTCTGTGTGGGTCGCCGTGCCTGCAGCTTTGAATCAAGTGGA GAAGCACTTCAAGGCTGGACAAAGTAAAGATTATTGTTATTTTTTTTCT TTCTCTTCCTCTCTTTTAAGAAAGGAAAATATTCCAAGGACTAATTTGG TCGTGTCTTCCTTCATGTAAGTACCTCTGACATTTTTCCAAAAGAATAG AAATAGCTTGTGTATTGTCTCTGAAATCTGCACCAATCTCTTCCAGGCA CTGGGTCTATCTATCCAACTCCTTTCTGGAAGGCTTAAGTTAAGGCTTG TTGTGCATTCTTTTCTTTAGACTCTACGATTTCCTTGTGTGTGTCTGAAA GTAACTTTTTAGATAGTAGTATCCGTTTGCCATCTGCTATTGAATTCAC ATCTGACTCTTCCTGTCACATCAGTTTGTTTAAAGTTTCAAGAAGTTAG TTCCTGTCATTAGCATGTTTGATAGGGTGGAGAACGTGGATACTAGTGT ATTTTAGGATTTCACAGACTGTTCTGTGACCTTGAAGTCGCTGTCTTAA AATTTAGCTCTTAGTTCACTGTGGAAAGATGTTCCTATGAGTTACCCCA AAGACTGGTTTTCCCTGGGTTTGGATTCTGAGCCA
Mef2c-ΔAR	ACACTTCGTCTCCAGCTCTCTGCTCGCTCGCCTCGCAGTCACAGACACT TGAGCACACGCGTACACCCAGACATCTTCGGGCTGCTATTGGATTGACT TTGAAGGTTCTGTGTGGGTCGCCGTGCCTGCAGCTTTGAATCAAGTGGA GAAGCACTTCAAGGCTGGACAAAGTAAAGATTATTGTTATTTTTTTTCT TTCTCTTCCTCTCTTTTAAGAAAGGAAAATATTCCAAGGACTAATTTGG TCGTGTCTTCCTTCATGTAAGTACCTCTGACATTTTTCCAAAAGAATAG AAATAGCTTGTGTATTGTCTCTGAAATCTGCACCAATCTCTTCCAGGCA CTGGGTCTATCTATCCAACTCCTTTCTGGAAGGCTTAAGTTAAGGCTTG TTGTGCATTCTTTTCTTTAGACTCTACGATTTCCTTGTGTGTGTCTGAAA GTAACTTTTTAGATAGTAGTATCCGTTTGCCATCTGCTATTGTGTCTTAA AATTTAGCTCTTAGTTCACTGTGGAAAGATGTTCCTATGAGTTACCCCA AAGACTGGTTTTCCCTGGGTTTGGATTCTGAGCCA
Mef2c-ΔMe	CGCCGTGCCTGCAGCTTTGAATCAAGTGGAGAAGCACTTCAAGGCTGG ACAAAGTAAAGATTATTGTTATTTTTTTTCTTTCTCTTCCTCTCTTTTAA GAAAGGAAAATATTCCAAGGACTAATTTGGTCGTGTCTTCCTTCATGTA AGTACCTCTGACATTTTTCCAAAAGAATAGAAATAGCTTGTGTATTGTC TCTGAAATCTGCACCAATCTCTTCCAGGCACTGGGTCTATCTATCCAAC TCCTTTCTGGAAGGCTTAAGTTAAGGCTTGTTGTGCATTCTTTTCTTTAG ACTCTACGATTTCCTTGTGTGTGTCTGAAAGTAACTTTTTAGATAGTAG TATCCGTTTGCCATCTGCTATTGAATTCACATCTGACTCTTCCTGTCACA TCAGTTTGTTTAAAGTTTCAAGAAGTTAGTTCCTGTCATTAGCATGTTTG ATAGGGTGGAGAACGTGGATACTAGTGTATTTTAGGATTTCACAGACT GTTCTGTGACCTTGAAGTCGCTGTCTTAAAATTTAGCTCTTAGTTCACTG TGGAAAGATGTTCCTATGAGTTACCCCAAAGACTGGTTTTCCCTGGGTT TGGATTCTGAGCCA
Mef2c-ΔARΔMe	CGCCGTGCCTGCAGCTTTGAATCAAGTGGAGAAGCACTTCAAGGCTGG ACAAAGTAAAGATTATTGTTATTTTTTTTCTTTCTCTTCCTCTCTTTTAA GAAAGGAAAATATTCCAAGGACTAATTTGGTCGTGTCTTCCTTCATGTA AGTACCTCTGACATTTTTCCAAAAGAATAGAAATAGCTTGTGTATTGTC TCTGAAATCTGCACCAATCTCTTCCAGGCACTGGGTCTATCTATCCAAC TCCTTTCTGGAAGGCTTAAGTTAAGGCTTGTTGTGCATTCTTTTCTTTAG ACTCTACGATTTCCTTGTGTGTGTCTGAAAGTAACTTTTTAGATAGTAG TATCCGTTTGCCATCTGCTATTG

Table S4 The sequences of shRNAs.

shRNAs	Sequence
Mef2c sh1	CGCCAGCACTGACATGGATAA
Mef2c sh2	CTCTGCAGAGGAATAGTATGT
Mef2c sh3	CTCACCTGGTAACCTGAACAA
Mef2c sh4	ATCAGTGAATCAAAGGATAAA